Cartesian Trajectory Based Control of Dobot Robot

Md Rasedul Islam, Md Arifur Rahaman, Md Assad-uz-Zaman, and Mohammad Habibur Rahman

BioRobotics Lab
University of Wisconsin-Milwaukee
Milwaukee, WI 53211, USA
islam4@uwm.edu, rahaman.arifur02@gmail.com, assaduz2@uwm.edu, rahmanmh@uwm.edu

Abstract

Dobot Magician-a 3 degrees of freedom (DoF) robot- is widely used nowadays in education and in research on industrial robotics. In this paper, we developed forward kinematics and inverse kinematics of Dobot magician robot, and built a non-linear approach for cartesian control of its end-effector position. Modified Denavit-Hartenberg (DH) convention was used to obtain forward kinematics. An Algebraic approach was used to find inverse kinematics solution and presented in details. An algorithm based on developed inverse kinematic was developed to conversion Dobot's Cartesian variables into joint variables. This conversion facilitated to obtain Cartesian control of Dobot Magician robot. Lastly, simulation results show stability and efficacy of developed control approach in maneuvering the Dobot's end-effector position.

Keywords
Dobot robot, Forward Kinematics, Inverse Kinematics, Cartesian Control, Trajectory Tracking

1.0 Introduction:

The use of robots has been increasing exponentially through the last couple of decades. Extensive research has been going on in the area of robot design and control to make such robots intelligent and to increase the performance of the robotic operation. The research includes the robot application in small/large industries for fine object manipulation (Wilson et al. 2016, Holz et al. 2015, Su et al. 2015), health care industries as an assistive device (Rabbitt et al. 2015, Vandemeulebroucke et al. 2018) and/or rehabilitation device (Nef et al. 2009, Cui et al. 2017, Islam et al. 2017, Assad-Uz-Zaman et al. 2016, Islam et al. 2019), mining/hazardous environment for safe handling/operation (Quintana et al. 2018, Bai et al. 2018), precision manufacturing, and STEM education (Li et al. 2018).

Dobot Magician (Shenzhen Co 2019a) is a commercially available lightweight, multifunctional desktop robotic arm that resembles a 3DOF industrial robotic manipulator is nowadays widely used for STEM education. Dobot users use 'Dobot Studio' (Shenzhen Co 2019b) software to program the Dobot for object manipulation. However, Dobot studio does not have resources to teach robot kinematics, dynamics, and simple control techniques such as PID control. There is a great potential to use the Dobot in undergraduate lab and teach robotics if its kinematics, dynamics, and control strategies can be formulated. Therefore, in this research we have developed Dobot's forward kinematics, inverse kinematics, dynamic modeling, and control technique using simple PID controller. It is anticipated that this research article will be a key learning resource for the undergraduate students and for researchers working on robotics especially with the Dobot Magician.

To develop the forward kinematics the well known modified Denavit Hartenberg conventions (Denavit and Hartenberg 1955) were used, and for the inverse kinematic algebraic approach was used. Note that for the Cartesian control of a robot it is essential to know the inverse kinematic solution of a robot. The recursive Newon-Euler formulation (Craig 2017) was used to develop the dynamic model of the robot. To demonstrate the control using PID technique, simulation was carried out in Simulink environment where the Dynamic model of the dobot was simulated to follow both joint space and cartesian space trajectories.

2.0 Dobot Configuration :

The Dobot is a 3 DoF robot that has three stepper motors to actuate its joints (base, shoulder and elbow). The payload capacity of Dobot's end effector is 500 gram. The end-effector uses a servo motor and a pneumatic pump to deal with payload. The maximum distance that can be reached by Dobot is 320 mm. It can work under the temperature range -10°C to 60°C. Its joints' range of motion and maximum speed are shown in **Table-1**.

Table 1. Joint Range of Motion and Speed

Axis	Range	Max Speed (250g workload)
Joint 1 base	-135° to +135°	320° /s
Joint 2 rear arm	0° to +85°	320° /s
Joint 3 forearm	-10° to +95°	320° /s

3.0 Forward Kinematics:

In this section, we present forward kinematics of Dobot Magician robot. To do so, the axes of joint-1, 2, and 3 are placed as shown in **Fig-1.** The Modified Denavit-Hartenberg (DH) method has been followed to assign the coordinate frame (Denavit and Hartenberg 1955, Craig 2017). To obtain the DH parameters, co-ordinate frames (i.e., the link-frames which map between the successive axes of rotation) are assumed to have coincided with the joint axes of rotation and have the same order. **Table-2** shows the DH parameters of the Dobot Magician robot.

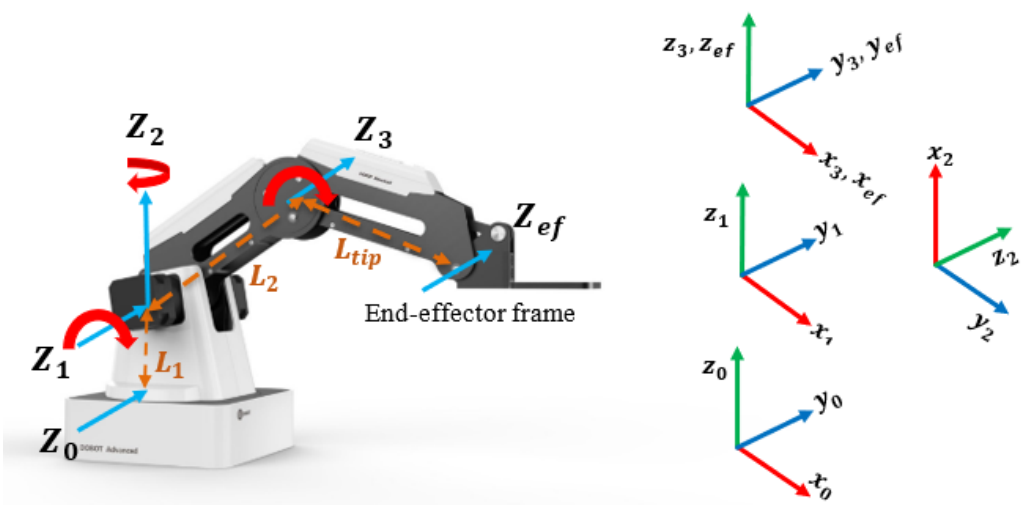

Figure 1: Coordinate frame assignment of Dobot magician robot

Table 2. Modified DH parameter of Dobot robot

Joint (i)	α_{i-1} (Link twist)	d_i (Link offset)	a_{i-1} (Link length)	q_i (Joint variable)
1	0	0	L_1	θ_1
2	$-\pi/2$	0	0	$\theta_2 - \pi/2$
3	0	L_2	0	θ_3
3	0	L_{tip}	0	0

We know that the general form of a link transformation that relates frame $\{i\}$ relative to the frame $\{i-1\}$ (Craig 2017) is:

$$ {}^{i-1}_{i}T = \begin{bmatrix} {}^{i-1}_{i}R^{3\times3} & {}^{i-1}_{i}P^{3\times1} \\ 0^{1\times3} & 1 \end{bmatrix} \tag{1} $$

where, ${}^{i-1}_{i}R$ is the rotation matrix that describes the frame $\{i\}$ relative to the frame $\{i-1\}$ and can be expressed as:

$$ {}^{i-1}_{i}R = \begin{bmatrix} \cos\theta_i & -\sin\theta_i & 0 \\ \sin\theta_i\cos\alpha_{i-1} & \cos\theta_i\cos\alpha_{i-1} & -\sin\alpha_{i-1} \\ \sin\theta_i\sin\alpha_{i-1} & \cos\theta_i\sin\alpha_{i-1} & \cos\alpha_{i-1} \end{bmatrix} \tag{2} $$

and, ${}^{i-1}_{i}P$ is the vector that locates the origin of the frame $\{i\}$ relative to the frame $\{i-1\}$ and can be expressed as:

$$ {}^{i-1}_{i}P = [a_{i-1} \quad -s\,\alpha_{i-1}\,d_i \quad c\,\alpha_{i-1}\,d_i]^T \tag{3} $$

Using equations (1) through (3) the single homogeneous transfer matrix that relates two successive frames (of figure) can be found as:

$$ {}^{0}_{1}T = \begin{bmatrix} \cos\theta_1 & -\sin\theta_1 & 0 & 0 \\ \sin\theta_1 & \cos\theta_1 & 0 & 0 \\ 0 & 0 & 1 & L_1 \\ 0 & 0 & 0 & 1 \end{bmatrix}, \qquad {}^{1}_{2}T = \begin{bmatrix} \sin\theta_2 & \cos\theta_2 & 0 & 0 \\ 0 & 0 & 1 & 0 \\ \cos\theta_2 & -\sin\theta_2 & 0 & 0 \\ 0 & 0 & 0 & 1 \end{bmatrix} $$

$$ {}^{2}_{3}T = \begin{bmatrix} \cos\theta_3 & -\sin\theta_3 & 0 & L_2 \\ \sin\theta_3 & \cos\theta_3 & 0 & 0 \\ 0 & 0 & 1 & 0 \\ 0 & 0 & 0 & 1 \end{bmatrix}, \qquad {}^{3}_{ef}T = \begin{bmatrix} 1 & 0 & 0 & L_{tip} \\ 0 & 1 & 0 & 0 \\ 0 & 0 & 1 & 0 \\ 0 & 0 & 0 & 1 \end{bmatrix}. $$

The homogenous transformation matrix that represents frame {ef} with respect to the frame {0} can be obtained by multiplying individual transformation matrices.

$$ {}^{0}_{ef}T = \left[{}^{0}_{1}T.\,{}^{1}_{2}T.\,{}^{2}_{3}T.\,{}^{3}_{ef}T\right] = \begin{bmatrix} r11 & r12 & r13 & Px \\ r21 & r22 & r23 & Py \\ r31 & r32 & r33 & Pz \\ 0 & 0 & 0 & 1 \end{bmatrix} \tag{4} $$

The equation obtained from this transformation matrix is known as the forward kinematic equation and is given below.

$$ \begin{aligned} r11 &= C_1C_2C_3 + C_1C_2S_3 \\ r12 &= C_1C_2C_3 - C_1S_2S_3 \\ r13 &= -S_1 \\ r21 &= S_1S_2C_3 + S_1C_2S_3 \\ r22 &= S_1C_2C_3 - S_1S_2S_3 \\ r23 &= C_1 \\ r31 &= C_2C_3 - S_2S_3 \\ r32 &= -(C_2S_3 - S_2C_3) \\ r33 &= 0 \\ Px &= L_2C_1S_2 + L_{tip}C_1(C_2S_3 + S_2C_3) \\ Py &= L_2S_1S_2 + L_{tip}S_1(S_2C_3 + C_2S_3) \\ Pz &= L_1 + L_{tip}(C_2C_3 - S_2S_3) + L_2C_2 \end{aligned} $$

Where, $cos\theta_1 = C_1,\ cos\theta_2 = C_2,\ cos\theta_3 = C_3,\ sin\theta_1 = S_1,\ sin\theta_2 = S_2,\ sin\theta_3 = S_3$

With the joint variable of each joint (θ_1, θ_2, and θ_3), using this forward kinematic equation, the position and orientation of frames were determined with respect to the reference frame.

4.0 Inverse Kinematic Solution:

From forward kinematics (equation (4)), we obtain the position of end-effector with respect to the base,

$$ {}^{0}_{ef}P = \begin{bmatrix} Px \\ Py \\ Pz \end{bmatrix} = \begin{bmatrix} x \\ y \\ z \end{bmatrix} $$

$$ L_2C_1S_2 + L_{tip}C_1(C_2S_3 + S_2C_3) = x $$

$$ L_2S_1S_2 + L_{tip}S_1(S_2C_3 + C_2S_3) = y $$

$$ L_1 + L_{tip}(C_2C_3 - S_2S_3) + L_2C_2 = z $$

From trigonometric identities, we know

$$ C_2S_3 + S_2C_3 = \sin(\theta_2 + \theta_3) = S_{23} $$

$$ C_2C_3 - S_2S_3 = \cos(\theta_2 + \theta_3) = C_{23} $$

Using the above identities, we have,

$$ L_2S_2 + L_{tip}S_{23} = \frac{x}{C_1} \quad \dots\dots\dots\dots (5) $$

$$ L_2S_2 + L_{tip}S_{23} = \frac{y}{S_1} \quad \dots\dots\dots\dots (6) $$

$$ L_1 + L_{tip}C_{23} + L_2C_2 = z \quad \dots\dots\dots\dots\dots\dots\dots . (7) $$

From $(6) - (5) =>$

$$ 0 = \frac{y}{S_1} - \frac{x}{C_1} $$

$$ => \frac{x}{C_1} = \frac{y}{S_1} \quad \dots\dots\dots (8) $$

$$ => \frac{S_1}{C_1} = \frac{y}{x} $$

$$ => \tan\theta_1 = \frac{y}{x} $$

$$ => \theta_1 = \arctan\left(\frac{y}{x}\right) $$

Rearranging equation (7), we get

$$ L_2C_2 + L_{tip}C_{23} = z - L_1 \quad \dots\dots\dots\dots\dots\dots\dots . (9) $$

Squaring both equation (5) and (9), and then by adding we obtain the following

$$ L_2^2S_2^2 + L_{tip}^2\, S_{23}^2 + 2L_2L_{tip}S_2S_{23} + L_2^2C_2^2 + L_{tip}^2\, C_{23}^2 + 2L_2L_{tip}C_2C_{23} = \left(\frac{x}{C_1}\right)^2 + (z - L_1)^2 $$

$$ => L_2^2(S_2^2 + C_2^2) + L_{tip}^2\,(S_{23}^2 + C_{23}^2) + 2L_2L_{tip}(S_2S_{23} + C_2C_{23}) = \left(\frac{x}{C_1}\right)^2 + (z - L_1)^2 $$

Where,

$S_2^2 + C_2^2 = 1,\ S_{23}^2 + C_{23}^2 = 1,$

$S_2S_{23} + C_2C_{23} = cos\,(\theta_2 + \theta_3 - \theta_2) = \ cos\theta_3 = C_3$

$p^2 = \left(\frac{x}{C_1}\right)^2 + (z - L_1)^2 = (x + y)^2 + (z - L_1)^2$

Therefore, we get

$=> L_2^2 + L_{tip}^2\ + 2L_2L_{tip}C_3 = p^2$

$$=> C_3 = \frac{p^2 - L_2^2 - L_{tip}^2}{2L_2L_{tip}}$$

So,

$$S_3 = \pm\sqrt{1-(C_3)^2}$$

$$=> \theta_3 = arc\tan\left(\frac{S_3}{C_3}\right) = arc\tan\left(\frac{\pm\sqrt{1-(C_3)^2}}{C_3}\right)$$

Now multiplying equation (5) by S_2 and equation (9) by C_2, we have

$$L_2S_2^2 + L_{tip}S_2S_{23} = \left(\frac{x}{C_1}\right)S_2 \quad \dots\dots\dots\dots\dots (10)$$

$$L_2C_2^2 + L_{tip}C_2C_{23} = (z - L_1)C_2 \quad \dots\dots\dots\dots\dots (11)$$

Adding equation (10) and (11), we have

$$L_2S_2^2 + L_2C_2^2 + L_{tip}S_2S_{23} + L_{tip}C_2C_{23} = \left(\frac{x}{C_1}\right)S_2 + (z - L_1)C_2$$

$$=> L_2(S_2^2 + C_2^2) + L_{tip}(S_2S_{23} + C_2C_{23}) = \left(\frac{x}{C_1}\right)S_2 + (z - L_1)C_2$$

$$=> L_2 + L_{tip}C_3 = \left(\frac{x}{C_1}\right)S_2 + (z - L_1)C_2$$

Let,

$$L_2 + L_{tip}C_3 = r\ , (z - L_1) = a, \left(\frac{x}{C_1}\right) = b$$

$$=> r = b\,S_2 + aC_2$$

$$=> r = a\cos\theta_2 + b\ \sin\theta_2 \quad \dots\dots\dots\dots\dots..(12)$$

Equation (12) is a transcendental equation. Therefore, we can solve it using half angle property of trigonometry,

Let,

$$u = \tan\frac{\theta_2}{2}, \cos\theta_2 = \frac{1-\tan^2\frac{\theta_2}{2}}{1+\tan^2\frac{\theta_2}{2}} = \frac{1-u^2}{1+u^2}\ \ , and\ \ \sin\theta_2 = \frac{2\ \tan\frac{\theta_2}{2}}{1+\tan^2\frac{\theta_2}{2}} = \frac{2u}{1+u^2}$$

Now using above identities, equation (12) becomes as follows,

$$r = a\left(\frac{1-u^2}{1+u^2}\right) + b\ \left(\frac{2u}{1+u^2}\right)$$

$$=> r(1+u^2) = a(1-u^2) + 2bu$$

$$=> (r+a)u^2 - 2bu + (r-a) = 0$$

This becomes a quadratic equation of variable *'u' with coefficients (r+a), (r-a), and -2b*. We can easily solve it.

$$u = \frac{2b \pm \sqrt{4b^2 - 4(r+a)(r-a)}}{2(r+a)}$$

$$=> u = \frac{2b \pm \sqrt{4b^2 - 4(r^2 - a^2)}}{2(r+a)}$$

$$=> u = \frac{2b \pm 2\sqrt{b^2 - (r^2 - a^2)}}{2(r+a)}$$

$$=> u = \frac{b \pm \sqrt{b^2 + a^2 - r^2}}{(r + a)}$$

$$=> \tan\frac{\theta_2}{2} = \frac{b \pm \sqrt{b^2 + a^2 - r^2}}{(r + a)}$$

$$=> \frac{\theta_2}{2} = arc\ tan\left(\frac{b \pm \sqrt{b^2 + a^2 - r^2}}{(r + a)}\right)$$

$$=> \theta_2 = 2\ arc\ tan\left(\frac{b \pm \sqrt{b^2 + a^2 - r^2}}{(r + a)}\right)$$

Therefore, we have a total four solutions (elbow up and down for joint-2 and joint-3).

$$[\theta_1, \theta_2, \theta_3] = \left[\arctan\left(\frac{y}{x}\right), \quad 2\ arc\ tan\left(\frac{b + \sqrt{b^2 + a^2 - r^2}}{(r + a)}\right), \quad arc\tan\left(\frac{+\sqrt{1 - (C_3)^2}}{C_3}\right)\right]$$

$$[\theta_1, \theta_2, \theta_3] = \left[\arctan\left(\frac{y}{x}\right), \quad 2\ arc\ tan\left(\frac{b + \sqrt{b^2 + a^2 - r^2}}{(r + a)}\right), \quad arc\tan\left(\frac{-\sqrt{1 - (C_3)^2}}{C_3}\right)\right]$$

$$[\theta_1, \theta_2, \theta_3] = \left[\arctan\left(\frac{y}{x}\right), \quad 2\ arc\ tan\left(\frac{b - \sqrt{b^2 + a^2 - r^2}}{(r + a)}\right), \quad arc\tan\left(\frac{+\sqrt{1 - (C_3)^2}}{C_3}\right)\right]$$

$$[\theta_1, \theta_2, \theta_3] = \left[\arctan\left(\frac{y}{x}\right), \quad 2\ arc\ tan\left(\frac{b - \sqrt{b^2 + a^2 - r^2}}{(r + a)}\right), \quad arc\tan\left(\frac{-\sqrt{1 - (C_3)^2}}{C_3}\right)\right]$$

Using these four solutions and workspace information of Dobot Magician, an algorithm for inverse kinematic solutions were developed in MATLAB.

5.0 Dynamics :

The dynamic equations of the proposed Dobot Magician robot have been derived from the iterative Newton-Euler formulation (Craig 2017).

$$\tau = M(\theta)\ddot{\theta} + V(\theta, \dot{\theta}) + G(\theta) \tag{13}$$

Where,

$M(\theta) \in \mathbb{R}^{3\times3}$ is the inertia matrix,
$V(\theta, \dot{\theta}) \in \mathbb{R}^3$ is the vector of centrifugal and Coriolis terms,
$G(\theta) \in \mathbb{R}^3$ is the gravity vector,
$\tau \in \mathbb{R}^3$ is the vector of joint torque.
$\theta \in \mathbb{R}^3$ is the vector of joint angle/position.
$\dot{\theta} \in \mathbb{R}^3$ is the vector of joint velocity.
$\ddot{\theta} \in \mathbb{R}^3$ is the vector of joint acceleration.

The iterative Newton-Euler equation for Dobot magician robot was coded as well as computed in MATLAB. The inertia matrix ($M(\theta)$), centrifugal and Coriolis vector ($V(\theta, \dot{\theta})$), and gravity vector ($G(\theta)$) are so large, hence they are not presented here.

6.0 Cartesian Control of Dobot robot:

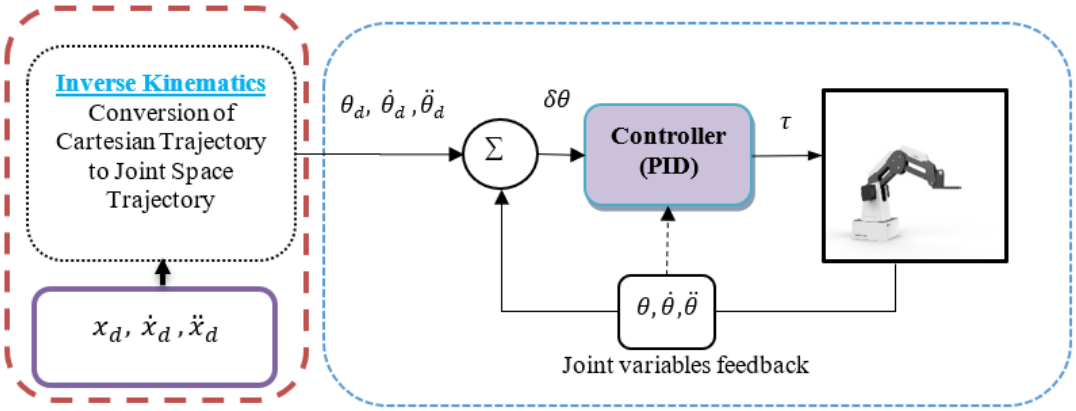

Figure 2. Cartesian trajectory tracking with joint based control

In Cartesian control of Dobot, the desired position (x_d), velocity ($\dot{x}_d$) and acceleration ($\ddot{x}_d$) of the Dobot's end-effector was given first. The inverse kinematics algorithm based on the inverse kinematic solution presented in section-4 was then used to convert the end-effector Cartesian variables (position, velocity, and acceleration) into joint variables (θ_d, $\dot{\theta}_d$, and $\ddot{\theta}_d$). After that, these joint variables were given as input to controller in the form of input trajectory. In this research, a PID control was used to obtain joint-based control of the Dobot Magician robot. The PID gain used in the controller were as follows: proportional Gain = diag(150 ,500,150); integral Gain = diag(0.1 , 0.1, 0.1); and derivative Gain = diag(10, 18, 10).

The controller estimates required joint torques to ensure Dobot's end-effector follow the desired position, velocity and acceleration. The general layout of the control architecture for 'Cartesian control of Dobot robot' is given in **Fig-2** where θ_d, $\dot{\theta}_d$, and $\ddot{\theta}_d$ represent desired joint angles, velocity and acceleration respectively. The inverse kinematic algorithm was developed in MATLAB (MathWorks, MA, USA) whereas control simulation was done in SIMULINK (MathWorks, MA, USA) respectively. In the simulation two cartesian trajectories (rectangular and circular path) were used to demonstrate the Caretican trajectory control of the Dobot robot using the developed inverse kinematics and the control approach.

6.1 Simulation-1:

In this simulation, a rectangular path was given as a reference trajectory to follow. To follow the given path, it requires Dobot's all three joints to move. The comparison between the reference trajectory and the measured (simulation output) trajectory (from simulation) is shown in **Fig-3**. It is clearly shown from the figure that measured path is almost overlapped with the reference path, which shows the effectiveness of the developed inverse kinematic algorithm and the controller. **Figure-4** shows the simulation result of the same experiment (i.e., tracking of a rectangular path) but was plotted in joint space, meaning all joints angle, velocity, and torque information. In **Fig-4**, the topmost graph shows the joint angle vs time plot; the 2nd row of the plot shows the tracking error (i.e., the difference between the reference angle and the measured angle) vs time; the 3rd row of the graph shows the joint velocity vs time; and the last row of the graph shows the joint torque vs time. From the **Fig-4** the maximum tracking error was observed around 0.5° which is very low and can be found for joint-3. This corroborates effectiveness of developed cartesian control approach for trajectory tracking.

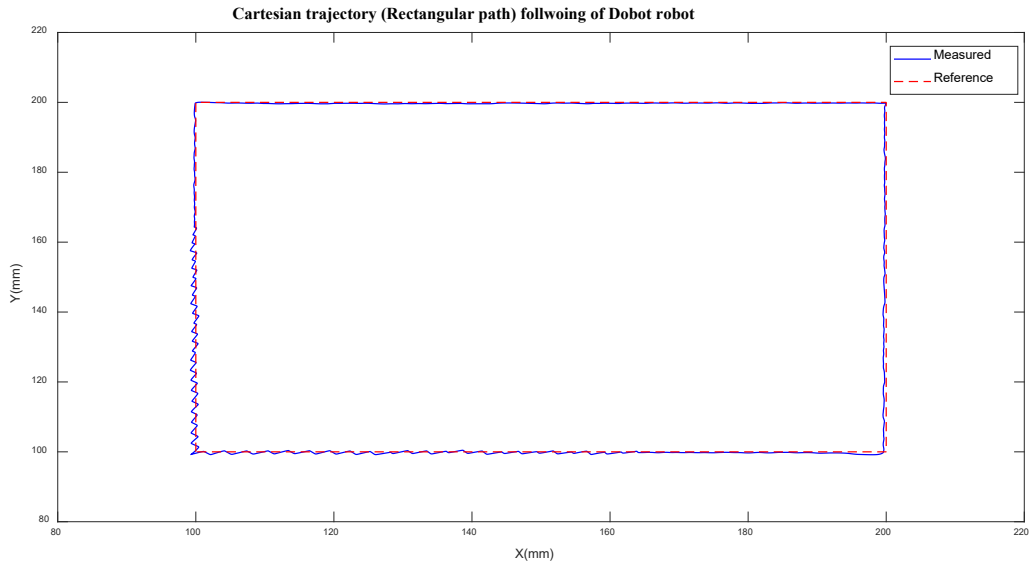

Figure 3.Comparison of rectangular reference path and corresponding measured **(**simulation output**)** the path

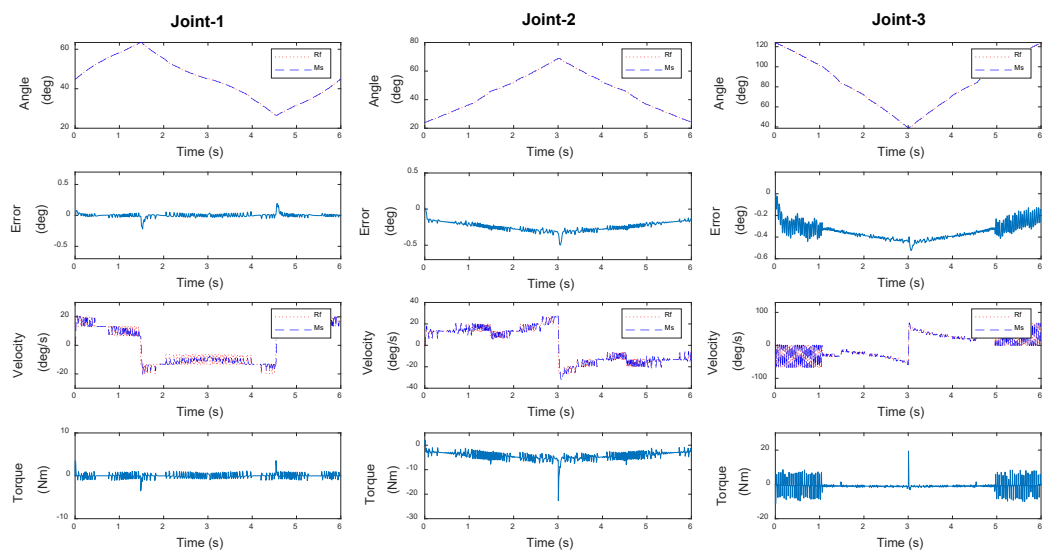

Figure 4. Simulation result of joints for rectangular path

6.1 Simulation-2:

In this simulation, a circular trajectory was given as reference and the center of the circle was coincident with the base frame of Dobot. Therefore, it was expected there would be only joint-1 movement while other two joints remain stationary.The comparison between reference trajectory and measured trajectory (from simulation) of circular path is shown in **Fig- 5**. It is clearly shown from the figure that measured path is almost overlapped with the reference path, which validates the developed inverse kinematic algorithm and also shows the performance of the controller to maneuver the Dobot effectively to follow the reference trajectory. **Figure-6** shows the simulation result of the same experiment (i.e., tracking of a circular path) but was plotted in joint space, meaning all joints position, velocity, and torque information. From **Fig-6** the maximum tracking error can be observed around 0.05° which is very low. This results further corroborates the effectiveness of developed cartesian control approach.

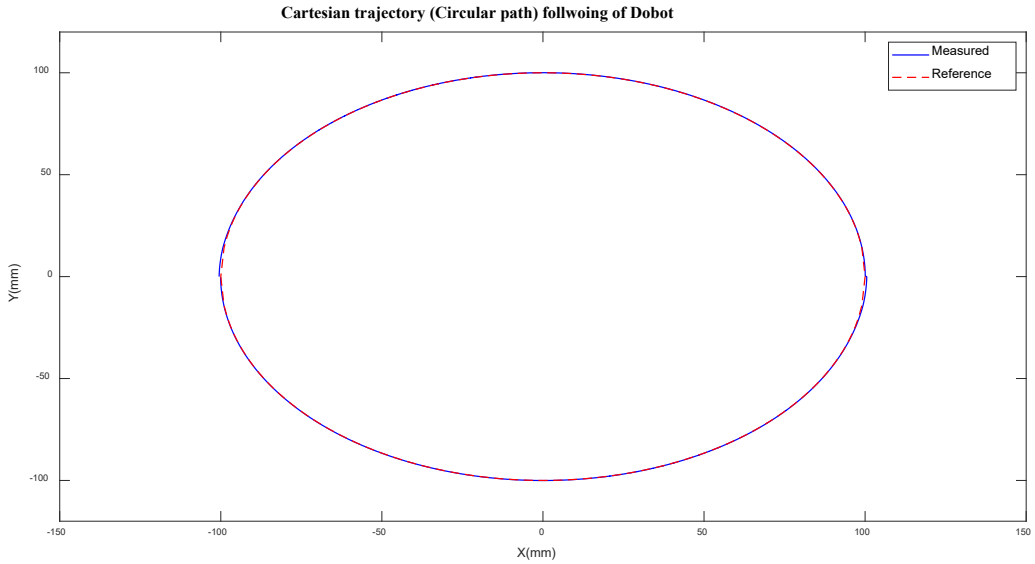

Figure 5. Comparison of circular reference path and corresponding measured path

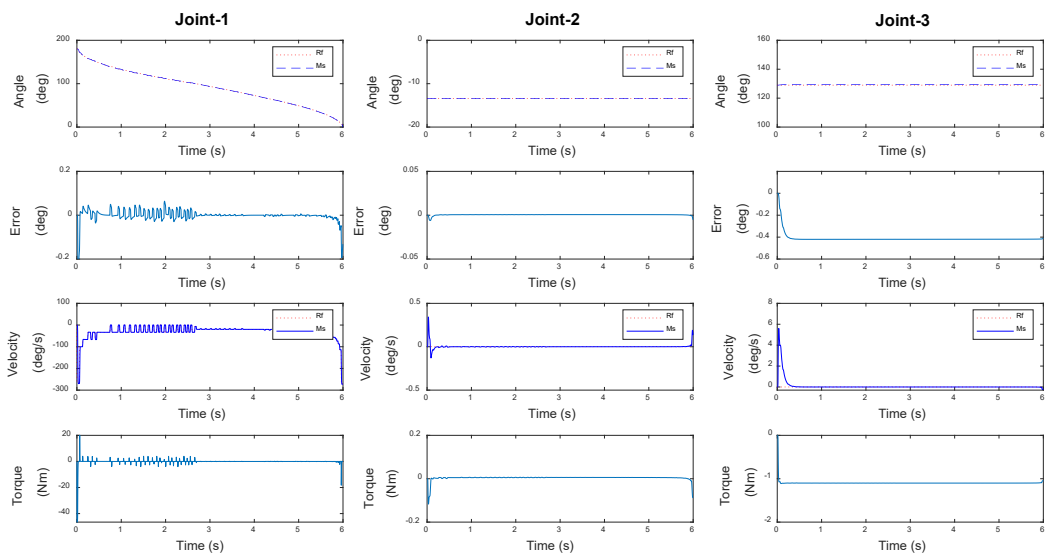

Figure 6. Simulation result of joints for a circular path

7.0 Conclusion:

In this paper, we have developed forward kinematics, inverse kinematics, dynamics of the Dobot Magician robot. An inverse kinematics algorithm was developed based on derived inverse kinematic solution. Finally, cartesian control of Dobot magician robot was accomplished with developed controller. The control simulation shows maximum error 0.5°. This controller will be further improved by adding a robust control (Sling mode control, Adaptive control etc.) to deal with the modeling uncertainties (future works).

References:

Assad-Uz-Zaman, M., Rasedul Islam, M., Miah, S., and Rahman, M. H., NAO robot for cooperative rehabilitation training, *Journal of Rehabilitation and Assistive Technologies Engineering, SAGE Publishing*, vol. 6, no. 1, pp. 1-14, 2019. doi: 10.1177/2055668319862151.

Bai, L., Guan, J., Xiaohong, C., Hou, J., Duan, W., An optional passive/active transformable wheel-legged mobility concept for search and rescue robots, *Robotics and Autonomous Systems*, vol. 107, no. 1, pp. 145-155, 2018.

Craig, J, J., *Introduction to Robotics: Mechanics and Control*, 4th Edition, Pearson, New Jersey, 2017.

Cui, X., Chen, W., Jin, X., Agrawal, S.K., Design of a 7-DOF Cable-Driven Arm Exoskeleton (CAREX-7) and a Controller for Dexterous Motion Training or Assistance, *IEEE/ASME Transactions on Mechatronics*, vol. 22. 6, no. 1, pp. 161-172, 2017.

Denavit, J., and Hartenberg, R, S., "A kinematic notation for lower-pair mechanisms based on matrices," *Trans. of the ASME. Journal of Applied Mechanics*, vol. 22, no. 1, pp. 215-221, 1955.

Islam, M.R., Spiewak, C., Rahman, M.H., and Fareh, F., A Brief Review on Robotic Exoskeletons for Upper Extremity Rehabilitation to Find the Gap between Research Porotype and Commercial Type, *Advances in Robotic and Automation*, vol. 6, no. 3, pp. 1-12, 2017, doi: 10.4172/2168-9695.1000177.

Islam, M.R., Assad-Uz-Zaman, M., and Rahman, M.H, Design and control of an ergonomic robotic shoulder for wearable exoskeleton robot for rehabilitation, *International Journal of Dynamics and Control, Springer Nature,*, pp. 1-14, 2019, doi: 10.1007/s40435-019-00548-3.

Li, C., Fu, L., Wang, L., Innovate engineering education by using virtual laboratory platform based industrial robot, *Proceedings of the Chinese Control And Decision Conference (CCDC)*, Shenyang, China, Jun 9 – 11, 2018.

Nef, T., Guidali, M., Riener, R., Agrawal, S.K., ARMin III-2013; Arm Therapy Exoskeleton with an Ergonomic Shoulder Actuation, *Applied Bionics and Biomechanics*, vol. 6, no. 2, pp. 127-142, 2009.

Holz, D., Topalidou-Kyniazopoulou, A., Rovida, M., Pedersen, R, M., Krüger, V., and Behnke, S., A skill-based system for object perception and manipulation for automating kitting tasks, *Proceedings of the IEEE 20th Conference on Emerging Technologies & Factory Automation (ETFA)*, Luxembourg, Sep 8 – 11, 2015.

Quintana, J., Garcia, R., Neumann, L., Campos, R., Weiss, T., Köser, K., Mohrmann, J., Greinert, J., Towards automatic recognition of mining targets using an autonomous robot, *Proceedings of the IEEE OCEANS MTS/IEEE*, Charleston, SC, Oct 22 – 25, 2018.

Rabbitt, S.M., Kazdin, A.E., and Scassellati, B., Integrating socially assistive robotics into mental healthcare interventions: Applications and recommendations for expanded use, *Clinical Psychology Review*, vol. 35, no. 1, pp. 35-46, 2015.

Shenzhen Yuejiang Technology Co. Ltd., Dobot Magician Specifications and Shipping List. *https://www.dobot.cc/dobot-magician/specification.html*. 2019a Accessed 29 Sep 2019

Shenzhen Yuejiang Technology Co. Ltd., Dobot Magician API Description. *https://www.dobot.cc/dobot-magician/specification.html*. 2019b. Accessed 29 Sep 2019

Spiewak, C., Islam, M.R., Rahman, M.A., Rahman, M.H., Smith, R., Modelling and control of a 4dof robotic assistive device for hand rehabilitation, *International Journal of Mechanical, Aerospace, Industrial, Mechatronic and Manufacturing Engineering*, vol. 10, no. 8. pp. 1372-1376, 2016.

SU, Y.H., Hsiao, C.C., Young, K.Y., *Manipulation System Design for Industrial Robot Manipulators Based on Tablet PC*, In: Liu H., Kubota N., Zhu X., Dillmann R., Zhou D. (eds) Intelligent Robotics and Applications. ICIRA. Lecture Notes in Computer Science, vol 9245. Springer, Cham, 2015.

Vandemeulebroucke, T., Casterlé, B., and Gastmans, C., How do older adults experience and perceive socially assistive robots in aged care: a systematic review of qualitative evidence, *Aging & Mental Health*, vol. 22, no. 2, pp. 149-167, 2018.

Wilson, J., Charest, M., and Dubay, R., Non-linear model predictive control schemes with application on a 2 link vertical robot manipulator, *Robotics and Computer-Integrated Manufacturing*, vol. 41, no. 1, pp. 23-30, 2016.

Biographies

Md Rasedul Islam is currently a PhD candidate in Mechanical Engineering department in University of Wisconsin – Milwaukee (UWM), USA. Mr Islam has been researching in wearable robotics intended to be used in rehabilitation of human upper limb of post-stroke patients. In addition, He has been working as a research assistant at Bio-Robotics lab here in UWM since August 2015. Mr Islam has been a Distinguished Graduate Student Fellowship and Distiguhsed Dissertation Fellow by UWM graduate school in 2017 and in 2018 respectively. Earlier, he has done his B.S in Mechanical Engineering from Khulna University of Engineering & Technology (KUET), Khulna, Bangladesh, in 2012. Soon after his B.S, he has joined as Lecturer in Mechanical Engineering in KUET.

Md Assad-Uz-Zaman (Ph.D student) at Bio-Robotics Lab, Mechanical Engineering Department, University of Wisconsin-Milwaukee, Milwaukee, WI USA. He received BSc Engineering (mechanical) from KUET, Khulna Bangladesh in 2013., a Master of Science (Mechanical Eng.) degree from University of Wisconsin-Milwaukee, USA in 2017. His research interests are in Portable rehabilitation device, Artificial Intelligence and Robot motion planning.

Mohammad Habib Rahman is with the Mechanical and Biomedical Engineering Department, University of Wisconsin-Milwaukee, WI, USA. As Director of the BioRobotics Lab at the University of Wisconsin-Milwaukee, he brings the resources and expertise of an interdisciplinary R&D team. For more than 15 years he has been researching bio-mechatronics/bio-robotics with emphasis on the design, development and control of wearable robots to rehabilitate and assist elderly and physically disabled individuals who have lost their upper-limb function or motion due to stroke, cardiovascular disease, trauma, sports injuries, occupational injuries, and spinal cord injuries. He received a BSc Engineering (mechanical) degree from Khulna University of Engineering & Technology, Bangladesh in 2001, a Master of Engineering (bio-robotics) degree from Saga University, Japan in 2005 and a PhD in Engineering (bio-robotics) from École de technologie supérieure (ETS), Université du Québec, Canada in 2012. He worked as a postdoctoral research fellow in the School of Physical & Occupational Therapy, McGill University (2012-2014). His research interests are in bio-robotics, exoskeleton robot, intelligent system and control, mobile robotics, nonlinear control, control using biological signal such as electromyogram signals.